Lithium-ion battery SoH estimation based on incremental capacity peak tracking at several current levels for online application

M. Maures, A. Capitaine, J.-Y. Delétage, J.-M. Vinassa, O. Briat

Lithium-ion battery SoH estimation based on incremental capacity peak tracking at several current levels for online application

M. Maures[a,*], A. Capitaine[a], J.-Y. Delétage[a], J.-M. Vinassa[a], O. Briat[a]

[a] *Univ. Bordeaux, CNRS, Bordeaux INP, IMS, UMR 5218, F-33400 Talence, France*

Abstract

In this paper, an extension to high C-rates of State of Health (SoH) diagnostic methods based on Incremental Capacity (IC) peak tracking is proposed. A set of eleven NCA Lithium-ion batteries who went under different ageing protocol is used. Charge and discharge cycles are performed at C/20, C/10, C/5 and C/2, and then used for IC analysis. Correlations between the variations of IC peaks and SoH are presented and modelized, and shown to be accurate estimators for all tested C-rates.

1. Introduction

The Lithium-ion battery market is reaching all-time highs as a result of strong demand from new renewable energy solutions, such as Electric Vehicles (EVs) and More Electric Aircrafts (MEAs) in the transportation sector, or grid battery storage in the energy sector.

Compared to other applications, batteries in those systems will face significantly harsher working conditions: higher power rates and larger temperature variations, both of which significantly contribute to the batteries degradation [1,2]. As such, it is necessary to keep track of their State of Health (SoH) and determine when their end of useful life (for a specified application) is met. The SoH is generally defined as the ratio between the maximum capacity of a battery at a given time over its initial maximum capacity [3].

Different estimation methods exist to quantify the SoH of the batteries [4]: capacity or impedance based, using relaxation voltage or based on Incremental Capacity (IC) or Differential Voltage (DV) curves.

IC analysis provides significant information regarding degradation modes [5,6] inside the battery as each peak results from a phase transition for the material inside it [7]. However, because of this, IC curves are generally obtained through very slow charges/discharges [8,9] which limits their practicality.

Still, estimation methods have been proposed to quantify the SoH of a battery based on the geometric properties of IC peaks. In particular, [8,9] have shown linear correlations between the positions of specific IC peaks and valleys with the SoH, while [8] has also shown logarithmic correlations between their amplitude and SoH. This can prove particularly useful for online estimations: since peaks appear for specific voltages, only partial charges or discharges are required to measure their properties and estimate the SoH. However, given the low current limitations mentioned before, such a partial charge or discharge could still take more than an hour before providing any significant result.

As such, this paper aims at extending the methods of SoH estimation through IC to higher C-rates as a mean to accelerate online estimations, which can be useful as a mean to accelerate experiments in a laboratory environment, or to provide faster accurate predictions in an embedded device, for example in an EV, were current IC estimators could require an entire day to provide a SoH estimation. The paper is divided as follows: first, the protocols and experimental results are presented. Then, the peaks of IC curves for each SoH and C-rate are shown and for each case, a SoH estimator is proposed. This estimator is then modelized for each SoH and C-rate. Finally, the perspectives and the conclusions are drawn.

2. Experiments

2.1. Protocol

The tests were performed at the Cacyssée platform at the IMS Laboratory of Talence. A set of eleven Samsung INR18650-25R cylindric 18650 cells were chosen for this test. They are made of a Graphite anode and an NCA (Nickel-Cobalt-Aluminium) cathode, and have a commercial capacity of 2.5 Ah. All the tests were performed at 25°C in a controlled

* Corresponding author. matthieu.maures@u-bordeaux.fr
Tel: +33 (5) 40 00 26 58

environment using a climatic chamber. The chosen cells were initially stored in a dedicated space and already featured different SoHs (ranging from 80% to 100%) prior to this study, following previous ageing tests performed at the platform. Their characteristics and ageing protocols are summed up in the Table 1.

Table 1.
SoHs of the cells and previous tests performed on them. Detailed information regarding their ageing protocols can be found in the text below.

Label	Q^{i}_{max} (mAh)	Q^{f}_{max} (mAh)	SoH (%)	Performed Experiments
Cell 1	2445	2445	100	Break-in then cycling from -20°C to 55°C
Cell 2	2453	2453	100	
Cell 3	2444	2444	100	
Cell 4	2484	2427	97.7	Calendar ageing at SoC 95% and -20°C
Cell 5	2454	2419	98.6	
Cell 6	2455	2412	98.3	
Cell 7	2508	2295	91.5	Calendar ageing at SoC 95% and 25°C
Cell 8	2499	2289	91.6	
Cell 9	2463	1946	79.0	Calendar ageing at SoC 95% and 55°C
Cell 10	2455	1943	79.1	
Cell 11	2449	1981	80.9	

More specifically, the cells 1, 2, and 3 were only used for a single test consisting of a break-in period (to maximize coulombic efficiency [10,11]) and seven charge/discharge cycles performed at a C/20 C-rate from -20°C to 55°C, resulting in a total of 11 cycles. Because this test was only performed once and was done at a low solicitation level, no ageing was measured on those cells hence an initial capacity Q^{i}_{max} equal to the final capacity Q^{f}_{max}.

The cells 4 to 11 however were used for calendar ageing. The detailed protocol includes no break-in period, but a preliminary check-up to determine their capacity followed by a full charge and short discharge to set them at a SoC of 95%. Several hours of calendar ageing were then performed on them. To assess the effect of temperature, cells 4 to 6 were aged at -20°C, cells 7 and 8 at 25°C and cells 9 to 11 at 55°C. Additionally, the ageing protocols at -20°C and 55°C were divided into two sub-protocols were cells 4, 9, and 10 underwent calendar ageing in Open Circuit Voltage (OCV) mode, while cells 5, 6, and 11 underwent calendar ageing in Constant Voltage (CV) mode to measure their leakage courant and study their self-discharge. Furthermore, check-ups were performed every 1000h on cells 7 and 8, and every 500h on cells 4 to 6 and 9 to 11. Similarly to the test presented in this paper, all the previous ageing tests were also preformed in a climatic chamber.

Although those experiments are not the focus of this paper, their description will be useful to explain possible differences in the behaviour of the cells sharing the same SoH in the later stages of this study.

The test protocol for this specific study consisted in a CC C/2 charge followed by 1.5h of relaxation. A complementary CC C/20 charge was then applied until the cell reached 4.2V. A CC C/20 discharge followed by 1.5h of relaxation and complementary CC C/20 discharge to 2.5V was performed to ensure the battery was fully discharged. The C-rates charges/discharges cycles were then performed, each of them consisting in a CC charge, a 1.5h relaxation, a complementary CC C/20 charge, a CC discharge, a 1.5h relaxation and a complementary CC C/20 discharge. The tested C-rates were C/20, C/10, C/5, and C/2. Since the tests are meant for IC studies, data points were recorded for every 1mV increment rather than equally spaced in time. This results in cleaner IC curves without resorting to filtering the data, a process which can sometimes result in erroneous data if performed incorrectly [12].

2.2. Results

At the end of the test, the charge and discharge curves for each SoH (Fig. 1) and C-rate (Fig. 2) can be plotted.

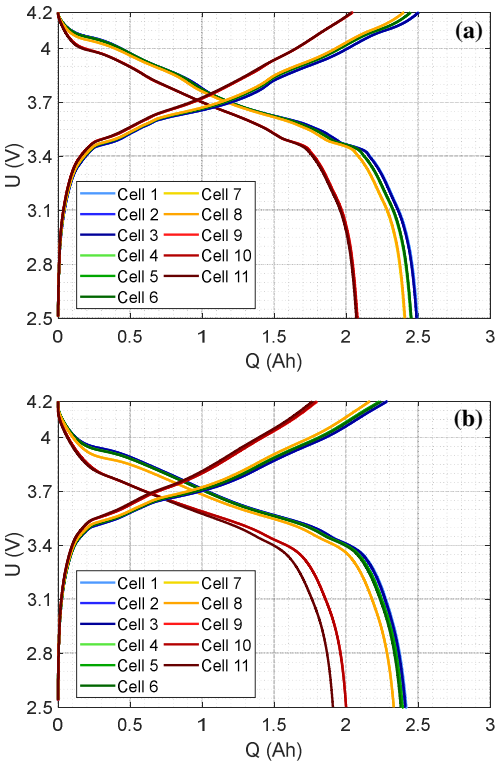

Fig. 1. Cell Voltage U vs Charge/Discharge Capacity Q for C/20 (a) and C/2 (b) C-rates, for the cells in Table 1. Cells 1,2, 3 are at a 100% SoH, cells 4, 5, 6 at a 98% SoH, cells 7, 8 at a 90% SoH, and cells 9, 10, 11 at an 80% SoH.

As shown in Fig. 1, for cells sharing the same

SoH, the charge and discharge curves generally coincide. The only exception is for the discharge curve of the cell 11, which deviates significantly from the two others at C/2. This effect is also noticeable at C/5 (see Fig. 2), but more noticeable at C/2. The effect is also seen at the end of discharge, at which the internal resistance of the cell is the highest, suggesting a higher increase in resistance for this cell compared to cells 9 and 10.

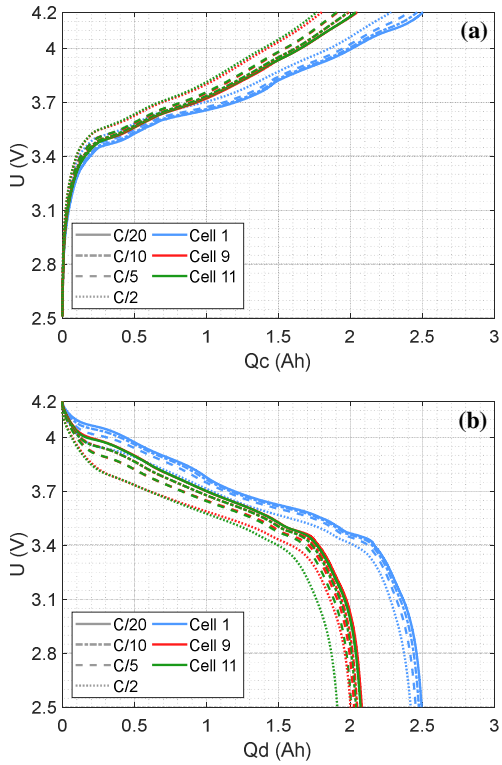

Fig. 2. Cell Voltage U vs Charge Capacity Q_c (a) and Discharge Capacity Q_d (b) for all C-rates. Given the proximity of the curves sharing the same SoH, only the data for the cell 1, cell 9, and cell 11 are represented. The deviation between cell 9 and cell 11 is clearly visible at C/2, which is not the case at lower C-rates.

This discrepancy can be explained by the differences in the ageing protocols compared to the other cells. Looking at cells 4, 5, and 6, there are no differences in the behaviour of the charge or discharge curves, despite cell 4 having a different protocol. This is because this ageing protocol was performed at low temperature (-20°C), at which the degradation is known to be weaker for calendar ageing [6]. This is especially true for resistance increase. On the other hand, at higher temperature (55°C), the degradations are accelerated.

Likewise, the SoC at which the calendar ageing is performed also contributes to accelerated or diminished degradations [13]. In the case of the tested cells, they were all charged at a 95% SoC before calendar ageing, however cells 5, 6, and 11 were also calendar ageing in CV mode. As such, they didn't self-discharge like the other cells and generally saw a slightly higher C-rates. Over the length of the test, this resulted in a higher resistance increase (see Table 2).

The difference between cell 11 and cells 9 and 10 is not of concern for the study however, as the proposed method only focuses on SoH as a ratio of capacities, which remain similar for those three cells.

Table 2.
Initial (R^i) and final (R^f) resistances of the cells following calendar ageing. The resistances were measured at SoC 50% with a 10s 1C current pulse.

Label	R^i (mΩ)	R^f (mΩ)	Increase (%)
Cell 4	26.4	27.0	2.4
Cell 5	26.5	27.4	3.7
Cell 6	26.4	27.5	4.2
Cell 9	26.3	39.1	48.3
Cell 10	26.5	39.3	48.3
Cell 11	26.6	41.9	57.6

2.3. Incremental Capacity (IC)

By differentiating the charged capacity over the voltage, the IC curves can also be plotted (see Fig. 3).

Looking at Fig. 3, the effect of SoH on the IC curves is clearly noticeable: as the cell degrades, the amplitude of the peak decreases. This is better seen at an 80% SoH where the peak at ~4.1V vanishes entirely. Additionally, it seems the peaks tend to move towards higher voltages. This is better seen on the peaks ① and ③. Meanwhile, the effect of C-rate is more subtle: position doesn't seem to be affected by the C-rate, while the amplitude of the peaks on the other hand is. This is because for a new cell and a given C-rate, the phase transitions during the charge or discharge process will always occur at the same time. Those phases transitions are associated to specific voltages, which are highlighted by the peaks of the Incremental Capacity curves [7]. These voltages are related to the positions of the peaks. When the C-rate increases, those phases transitions still occur for the same voltages, hence a minimal effect on the peak position. However, as the C-rate increases, the internal impedance of the cell leads to more Joule losses, and in general, a higher voltage drop. This means the cell will reach its end voltage in a faster time, but also with less actual charges (hence less capacity). The total number of charges in the cell is the area below the Incremental Capacity curve, where each phase transition will move a certain amount of charge [14]. This area depends on the width and the height of the peaks, and so, as the total number

of charges inside the cell decreases, so will the peaks' heights.

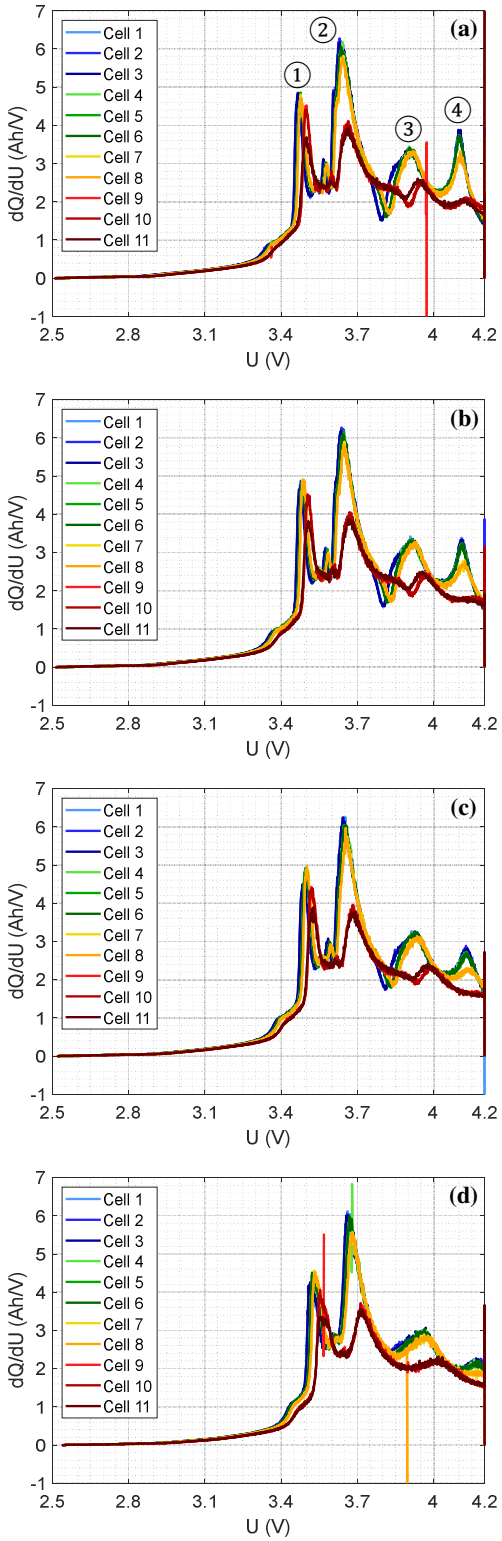

Fig. 3. IC of the charge curves for all the cells at C/20 (a), C/10 (b), C/5 (c), and C/2 (d).

Nevertheless, the hierarchy between the peaks remains the same for all C-rates, suggesting the SoH should be quantifiable with correlation methods both for low C-rates and high C-rates.

These observations can also be made on the discharge curves, although in this case the peak ④ is significantly higher and usable for SoH estimation.

It should be noted that during all those tests, the temperature elevation never exceeded 3.25°C. As a result, it can be assumed the temperature will not affect the peaks' geometry significantly. This is also backed up by previous work performed at the platform were the heights, positions and widths or the peaks have been modelized and their evolutions plotted against temperature (see Fig. 4).

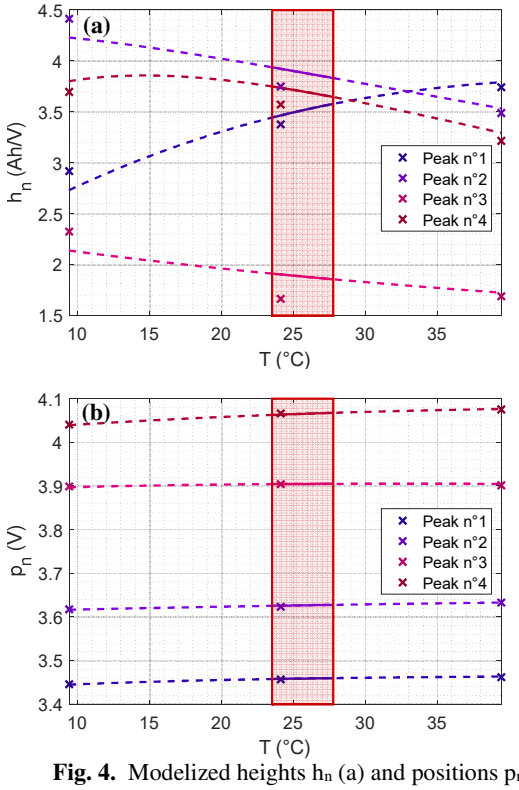

Fig. 4. Modelized heights h_n (a) and positions p_n (b) of modelized IC peaks from discharge curves performed on new cells at C/20 and temperatures ranging from -20°C to 55°C. Only the data from 10°C to 40°C is shown for clarity. The red area corresponds to the temperature variation underwent by the cells in this paper. Its effect on heights and positions is negligible (variation under 4%).

Essentially, the test was the one previously performed on cells 1 to 3 and described in part 2.1. The resulting data from those charges and discharges was used for IC modelization using four peaks, where the peaks' geometric properties were then plotted against temperature (see Fig. 4).

As it can be seen, both the heights and positions

are independent from temperature for small variations around 25°C, as even with a model (a modified Arrhenius law fitted from -20°C to 55°C, but whose description and fitting process is outside the scope of this paper), their variation is always less than 4%.

3. State of Health estimation

SoH estimation is generally performed by correlating a specific peak property with the SoH. In this study, correlations of all peaks positions and heights are tested for all charge and discharge IC curves, and for all C-rates, however, not all of them prove useful. Nevertheless, two estimators can be used, which share the same model versus SoH, and are represented in Fig. 5. A logarithmic regression was chosen for fitting purpose, based on previous literature studies [8]:

$$h_2 \text{ or } p_4 = a.\ln(SoH - b) + c \qquad (1)$$

where: h_2 is the height of the second peak, p_4 is the position of the fourth peak, and a, b, and c are model parameters.

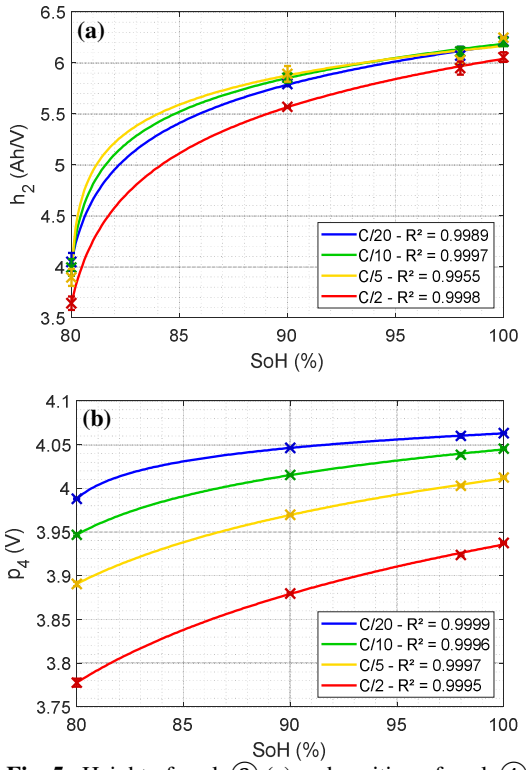

Fig. 5. Height of peak ② (a) and position of peak ④ (b) vs. SoH for all C-rates. The model (line) is based on Eq. 1. The crosses represent the averaged experimental data from cells sharing the same SoH, with error bars to highlight the deviation from each cell from the average. The relatively small error bars suggest good accuracy of the model.

Note that both peak parameters are not useful at the same time. The important differences between the charge and discharge IC curves means both processes need to be treated separately. In our case, h_2 is based on IC charge curves and p_4 on discharge curves. It should be noted that not using each estimator for the correct data set can lead to extremely erroneous results. For example, using p_4 on a charge IC curve can predict a SoH well above 100%, even for an aged cell. As such, only h_2 is suitable for SoH predictions on charge data sets, and only p_4 is suitable for predictions on discharge data sets. This is not a problem however, since h_2, although locally centred, will always be seen during the span of a full charge, while p_4 on the other hand is close to the end voltage, meaning only a small discharge is required for SoH estimation. Furthermore, as seen in Fig. 5., both parameters correlate well ($R^2 > 0.995$) for all C-rates, meaning the estimation of SoH can be performed very quickly without degrading the accuracy of the SoH prediction compared to other existing estimators [7,8]. For example, using a C/2 discharge and p_4, the SoH of a battery could be given in less than an hour.

Conclusion and perspectives

In this paper, a SoH estimator for several current levels is presented. The estimator is constructed using data from NCA cells whose SoH ranges from 100% (new) to 80%, tested on charge and discharge cycles performed at current levels ranging from C/20 to C/2.

The IC curves were constructed using voltage steps recordings, resulting in usable unfiltered data. While the effect of SoH was clearly visible on those curves, with more degraded cells presenting smaller peaks, the effect of C-rate was less noticeable. In particular, the hierarchy between the peak heights and positions with respect to SoH was the same at all tested C-rates.

The effect of temperature was also presented to assess the validity of the proposed method, as higher C-rates generally imply higher self-heating from the cells. It was shown that the temperature elevation was reasonably small to neglect the effect of temperature of both the peaks' heights and positions.

Although many parameters might be used for SoH estimation, two were extracted from IC curves and showed logarithmic correlations with SoH, both during charge and discharge. The correlations remain valid for C-rates as high as C/2, which help reducing testing time compared to traditional C/20 (or lower) IC studies, as well as providing opportunities to IC usage in an online application. Further work includes presenting the method for other current levels as well as other SoHs.

References

[1] J. Vetter et al., *Journal of Power Sources*, vol. 147, pp. 269–281, 2005.
[2] C. R. Birkl et al., *Journal of Power Sources*, vol. 341, pp. 373–386, 2017.
[3] D. Andre et al., *Journal of Power Sources*, vol. 224, pp. 20–27, 2013.
[4] K. Qian et al., *Electrochimica Acta*, vol. 303, pp. 183–191, 2019.
[5] C. Pastor-Fernández et al., in *6th Hybrid and Electric Vehicles Conference (HEVC 2016)*, 2016.
[6] M. Maures et al., *Microelectronics Reliability*, vol. 100–101, 2019.
[7] M. Dubarry et al., *J. Power Sources*, vol. 196, no. 23, pp. 10328– 10335, 2011.
[8] Y. C. Zhang et al., *Microelectronics Reliability*, vol. 88–90, no. July, pp. 1231–1235, 2018.
[9] Y. Li et al., *J. Power Sources*, vol. 373, no. November 2017, pp. 40– 53, 2018.
[10] M. Kassem and C. Delacourt, *J. Power Sources*, vol. 235, pp. 159–171, 2013.
[11] E. Redondo-Iglesias et al., *IEEE Trans. Veh. Technol.*, vol. 67, no. 1, pp. 104–113, 2018.
[12] X. Li et al.," *Appl. Energy*, vol. 177, pp. 537–543, 2016.
[13] Y. Gao et al., *J. Power Sources*, vol. 400, no. October, pp. 641–651, 2018.
[14] A. Barai et al., *Prog. Energy Combust. Sci.*, vol. 72, pp. 1–31, 2019.